Extracellular Caspase-1 regulates migration of hair follicle stem cells upon wounding

Subhasri Ghosh[1], Neha Pincha[1,2] , Akhil SHP Ananthan[1] , Sunny Kataria[1] , Rakesh Dey[1] , Srilekha Athreya [1,3], Colin Jamora[1].

Correspondence should be addressed to: colinj@instem.res.in, subhasri@instem.res.in

Affiliations :

1. IFOM - inStem Joint Research Laboratory, Institute for Stem Cell Biology and Regenerative Medicine, Bangalore, Karnataka, India
2. Manipal Academy of Higher Education, Manipal, Karnataka, India.
3. St. Joseph's College (Autonomous), Bangalore, Karnataka, India.

Abstract:

Migration of stem cells from one niche to another is a fundamental behavior observed during developmental processes such as organ specification and in homeostasis such as tissue regeneration and wound healing. A common theme running throughout these phenomena is the ability of cells to communicate with their environment to direct these stem cells to a specific location at a specific time. Deregulation of such cellular responses can lead to conditions such as developmental defects, tumor metastasis and ineffective wound closure. Wound healing is a physiological process that is activated upon tissue damage, which involves activation and migration of various cell types leading to the repair of the wounded tissue. In the context of the skin, wounding activates various resident stem cell pools including multipotent hair follicle stem cells, but how these cells are mobilized and directed to the damaged area has been an intractable problem for almost two decades. Wounded keratinocytes activate and secrete Caspase-1, a cytosolic protein well known as a critical regulator of inflammation. Surprisingly, we find that extracellular caspase-1 has a non-catalytic role of activating chemotaxis of

hair follicle stem cells into the wound bed. This exemplifies a novel function of an inflammatory molecule in recruiting adult stem cells that may underlie the epithelial hyperplasia found to accompany many inflammatory diseases.

Introduction:

Tissue damage necessitates the onset of healing mechanisms which involve rapid cellular regeneration by activating stem cell pools. The skin being the outermost protective barrier of our body has evolved the ability to heal itself rapidly owing to proliferation and migration of resident stem cell pools into the wound microenvironment (1). Wounding initially activates immune cells which infiltrate into the wound-bed and release cytokines and growth factors marking the inflammatory phase. This creates a foundation to support the ensuing proliferative phase during which neighboring stem cells proliferate and migrate into the wound to aid in rapid tissue formation and wound closure (2).

Reformation of the epidermal barrier by proliferation and migration of keratinocytes, known as re-epithelialization, is enhanced by the contribution of hair follicle stem cells (HFSCs) differentiating to epidermal keratinocytes, an emergency response not observed otherwise in homeostasis (1). Though wound directed migration of HFSCs had been first observed more than a decade ago, the guidance cues have remained elusive (3). It is becoming increasingly clear that inflammatory signals from resident and recruited immune cells are a major regulator of HFSC behavior in both homeostasis and wound-healing (4, 5). Interestingly this leukocyte-stem cell crosstalk is emerging as a common theme for the regulation of stem cells in a variety of niches (5). Therefore, identification of an unexpected migratory stimulus arising from an inflammatory signaling cascade is relevant not only in the context of wound healing but also skin carcinomas where physiological response mechanisms of epithelial stem cells are usurped (6). Our findings reveal a novel function of a common inflammatory molecule in directed cell migration.

Results:

Migration of hair follicle stem cells into the epidermis is recapitulated in a genetic model of wound healing

The physiological process of wound-healing is normally restricted to a small region proximal to the wound; for example in the skin, the activation of HFSCs is observed within less than a millimeter wide zone around the site of injury (3). This limits the number of responding cells, which has proven to be a formidable obstacle to deciphering the molecular mechanisms regulating this process. A genetic model that bypasses the need to induce a physical wound and simultaneously elicits a whole skin wound-healing reaction, amplifies the cellular crosstalk and signaling readouts that circumvents this technical hurdle. Here, we analyse the signaling mechanism in the conditional epidermal Caspase8 knock-out mouse (C8cKO) which recapitulates many of the hallmark features of wound-healing throughout the whole skin of the animal (7) and compare our observations to an excisional wound. Importantly, we find that HFSC chemotaxis to the wounded epidermis is also recapitulated in the C8cKO mouse skin, similar to that observed from a wound proximal hair follicle (Fig 1). HFSCs are marked by the expression of the transcription factor Sox9, a critical determinant of its stem cell identity and a widely used HFSC biomarker (8, 9). With this bona-fide marker we have traced the localization of HFSCs in unwounded to wounded conditions (Fig 1A) and between wild-type (WT) and C8cKO mice of postnatal age 4 days (p4) and 6 days (p6) (Fig 1B). Within 24 hours of wounding, HFSCs migrate out of the hair follicle and their numbers increase in the epidermis over 72 hours (Fig 1A). To evaluate change in the HFSC localization in C8cKO skin in comparison to WT p4 (Fig 1B) animals, the density of Sox9+ nuclei along hair follicles upto the epidermis was measured (Figure S1). Distribution analysis of their spatial density (represented as a heat map) clearly reveals an upward migratory trend towards the epidermis in the C8cKO skin compared to their WT counterpart at p4 (Fig 1C). Therefore, the HFSCs have started migrating even before epidermal hyperplasia has set in at p4. By p6, the HFSCs have already populated the epidermis of the C8cKO skin (Fig 1D). Gene expression changes in HFSCs upon wounding was analysed from published dataset collected from in vivo isolated HFSCs (10). This reveals a significant proportion of genes

classified under the category of regulation of cell migration (Figure S2). Select genes from this category were tested for their expression change upon wounding (Fig 1E) and in the epithelial compartment of the C8cKO skin from p4 mice (Fig 1F). We observed an increased expression of these genes via qPCR upon wounding and in the C8cKO epithelial compartment, thus validating the C8cKO genetic model as a platform to investigate the mechanisms guiding the directed epidermal migration of HFSCs upon wounding.

HFSC migration to the epidermis is regulated by soluble chemotactic cues.

We hypothesized that a chemotactic factor released from wounded or C8cKO epidermal keratinocytes would recruit HFSCs to the epidermis. To test if soluble mediators released from our genetic model of cutaneous wound healing can activate HFSC migration, conditioned media prepared from the epidermis (epiCM) was tested for its HFSC chemotactic properties by in vitro transwell migration assays. In comparison to WT epiCM, C8cKO epiCM can enhance the migration of HFSCs (Fig 2A). Interestingly, this effect was not manifested with primary epidermal keratinocytes (Fig 2B), suggesting that the soluble chemotactic factor(s) may be specific for mobilizing the HFSCs. Keratinocyte stress such as upon wounding or UV irradiation causes the release of a sleuth of intracellular proteins including pro-inflammatory cytokines, a prominent one of which is IL-1α. This release is mediated by the activation of Caspase-1 within an inflammosome complex inside the cells (11, 12) . An often overlooked fact is that Caspase-1 is also released under such conditions by an unconventional secretion route. We have also previously observed that Caspase-1 can be detected in the C8cKO epiCM in both the full-length and active forms (7) but in all these scenarios the function of the secreted protein is largely unknown. The release of IL-1α from wounded keratinocytes is required to mediate an epithelial-mesenchymal crosstalk which impacts the proliferation of HFSCs (4) but does not affect the migration of HFSCs (Fig 2C). The process of re-epithelialization is dependent on the migration of keratinocytes, thus any factor causing delay in migration of epidermal keratinocytes and HFSCs into the epidermis, can cause delay in wound healing. Caspase-1 null mice show delayed wound-

healing, where slower re-epithelialization is one of the causes (11, 13). Interestingly, the same defect is not recapitulated upon blocking the catalytic activity of caspase-1 (14) suggesting a signaling pathway where non-canonical role of Caspase-1 contributes to wound-healing. Taking into account these observations along with the release of extracellular Caspase-1 from wounded keratinocytes, we hypothesized that the extracellular Caspase-1 may function as the wound derived HFSC specific chemotactic factor.

Caspase-1 regulates the migration of HFSCs:

To determine the necessity of Caspase-1 specifically in HFSC migration we analyzed this process upon wounding the Caspase-1 null mice. HFSCs migrate out of wound-proximal hair follicles within 24 hours of wounding and populate the epithelial tongue (Fig 3A). In Caspase-1 null wounds, we find fewer Sox9+ cells as compare to wild-type demonstrating that loss of Caspase-1 delays HFSCs recruitment to the wounded epidermis. (Fig 3B). The same is reflected upon the expression analysis of the wound induced HFSC specific migration genes which show weaker upregulation in comparison to wild-type wounds (Fig 3C). Therefore, caspase-1 is necessary to initiate a robust migratory response in HFSCs upon wounding. Next, we probed whether Caspase-1 loss in the C8cKO mice shows a similar effect as in the excisional wound. HFSC distribution along hair follicles in wild-type, C8cKO and C8cKO-Casp1null p4 mice was analysed (Fig 3D). The heat map showing their distribution probability (Fig 3E), shows a shift towards the epidermis in the C8cKO which is rescued to the WT levels in the Caspase-8/Caspase-1 double knock-out (C8cKO-Casp1null). This loss in epidermal homing is due to the loss of Caspase-1 from the conditioned media, evident from the loss in chemotaxis of HFSCs to the C8cKO-Casp-1 null epidermal conditioned media (Fig 3F). Interestingly, the same effect is not observed upon blocking the catalytic activity of extracellular caspase-1 in the C8cKO epiCM using a non-cell permeable inhibitor of Caspase-1 (Fig 3G). Therefore, we infer that extracellular caspase-1 may have a novel, non-catalytic function in inducing the epidermal homing of HFSCs.

Recombinant Caspase-1 is sufficient to induce HFSC migration to the epidermis:

To test whether Caspase-1 is sufficient to induce HFSC migration we examined the chemotactic potential of bacterially expressed full-length murine Caspase-1. Caspase-1 activation involves autoproteolysis of the protein into the N-terminal CARD, a p20 and a p10 subunits upon association with the inflammosome The p20 and p10 subunits associate to form the catalytically active enzyme that can cleave downstream targets (15, 16) . Murine caspase-1 protein constructs having wild-type function (WT) and mutants which are catalytic dead (rCasp-1 CD) and proteolytic dead (rCasp-1 PD) (17) were bacterially expressed and partially purified by affinity chromatography (Figure S3A). These proteins were tested for their chemotactic effect on HFSCs in comparison to proteins isolated from bacteria transformed with empty vector (Fig 4A). Both the WT and the mutants showed equal potential to drive HFSC chemotaxis supporting our pharmacological data, that the canonical catalytic function is dispensable for caspase-1 to function as a HFSC chemoattractant. Moreover, Caspase-1 (rCasp-1 CD) is able to elicit this response in vitro independent of the proliferation status of the HFSCs as upon treating them with Mitomycin C, there was no loss in migration in comparison to proliferating cells (Fig 4B). We found that the chemotactic effect of the rCasp-1 CD protein is specific to HFSCs as primary keratinocytes do not show chemotaxis (data not shown). To test whether Caspase-1 is sufficient to induce migration of HFSCs from their niche in the skin, we treated Caspase-1 null skin explants with the r-Casp-1 CD. In comparison to vector treated, rCasp-1CD elicited migration of HFSCs to the epidermis (Fig 4C). To identify the chemotactically active domain of Caspase-1, the CARD and p-20 domain (C284A) were bacterially expressed and purified (Figure S3B) then tested in vitro for eliciting HFSC migration (Fig 4D). Our assay reveals that the chemotactic potential is held in the p-20 domain. Currently, we are testing the potential of this domain to function as a HFSC chemoattractant ex vivo and in vivo in Caspase-1 null mice. Therefore, we have demonstrated that Caspase-1 is the chemotactic factor that drives directional migration of HFSCs to the epidermis.

Discussion:

The migration of cells in response to a directional cue requires the ability of the cell to sense this cue and polarize its cytoskeleton and migratory machinery (18). Stem cell migration upon wounding is expected to utilize similar mechanisms but identification of the guidance cue was limiting. Our findings show that extracellular caspase-1 released from keratinocytes upon wounding activate the migratory response in adult stem cells of the skin, specifically the hair follicle stem cells. Caspase-1 activation is correlated to inflammatory signaling and persistent inflammation is thought to be a critical determinant of malignant transformation. Therefore, the unconventional secretion of caspase-1 along with other molecules must confer signaling specificity and regulate the outcome. Earlier studies have shown that wound-directed HFSC migration involves microtubule polarization regulated by GSK-3β (19) thus it remains to be tested whether Caspase-1 is regulating this signaling pathway and if so, identify the receptor.

Further investigation is required to probe whether caspase-1 is generic to activation of other stem cell populations present within the hair follicle, sebaceous glands and sweat glands upon wounding and in the development of skin carcinomas arising from hair follicle stem cells. Inflammatory conditions of the skin such as UV stress, psoriasis or atopic dermatitis is marked by caspase-1 activation and inflammatory cytokine release but what role the extracellular caspase-1 plays in these conditions need to probed. We must emphasize that in Caspase-1 null mice there is a delay in HFSC recruitment to the epidermis but it is not totally abrogated, suggesting the presence of other caspase-1 independent cues that may regulate stem cell migration.

Figure legends:

Figure 1: Epidermal knock-out of Caspase-8 recapitulates HFSC migration to the epidermis:

A) Localization of HFSCs based on Sox9 staining (red) in hair follicle and epidermis marked by keratin-5 (green) in unwounded and wounded skin at 24, 48 and 72

hours post wounding. There is an increase in the number of HFSCs in the infundibulum and epidermis over this time.

B) Panel showing HFSC localization in the skin of wild-type (WT) and Caspase-8 conditional knock-out (C8cKO) mice of age postnatal day 4 (p4) and postnatal day 6 (p6).

C) Density distribution of HFSCs along hair follicles from the epidermis represented as a heat-map. Samples obtained from WT and C8cKO skin from p4 mice.

D) HFSC numbers analysed from 50 by 50 μm^2 boxes in the epidermis of WT and C8cKO mice at p6.

E) Expression analysis of HFSC specific wound activated migration genes from unwounded (blue bar) and wounded skin (24 hours post wounding, red bar).

F) Expression analysis of same genes from WT epithelial cells (WT, blue bar) and C8cKO epithelial cells (C8cKO, red bar).

All data is represented from n=3 animals of each genotype. Error bars represent S.E.M. Scale bar= 30 μm.

Figure 2: HFSC migration to the epidermis is mediated by soluble chemotactic cues

A. Analysis of HFSC migration in a transwell Boyden chamber assay to C8cKO epidermal conditioned media (C8cKO epi CM) in comparison to the WT epi CM.

B. Analysis of migration in primary mouse keratinocytes to C8cKO epi CM in comparison to WT epi CM.

C. Analysis of HFSC migration to rhIL-1α. Positive control in B and C is J23T3 feeder cell conditioned media used traditionally as an inducer of HFSC migration (19) .

All data is represented from n=3 experiments. Error bars represent S.E.M.

Figure 3: Caspase-1 regulates HFSC migration to the epidermis

A. Panel showing HFSC (labeled with Sox9, red) migration into the epidermis from wound-proximal hair follicle 24 hours post wounding in wild-type (WT) and Caspase-1 null (Casp-1 null) mice.

B. Quantification of migrated HFSCs into the epithelial lip at 24 hours post wounding in WT (blue) and Casp-1 null (red) wounds from 100 by 100 μm^2 boxes.
C. Expression analysis of HFSC specific migration genes in wound samples from WT and Casp-1 null 24 hours post wounding.
D. Panel showing the localization of HFSCs (Sox9, red) in WT, C8cKO and C8cKO-Casp-1 null skin at p4.
E. Density distribution of HFSCs along hair follicles from the epidermis analysed from WT, C8cKO and C8cKO-Casp-1 null skin from p4 mice.
F. Analysis of HFSC chemotaxis to WT epiCM, C8cKO epiCM and C8cKO-Casp-1 null epiCM. Mean and S.E.M of n=2.
G. Analysis of HFSC chemotaxis to WT epiCM, C8cKO epiCM and C8cKO epiCM treated with Caspase-1 catalytic inhibitor (cell impermeable).

All data is representative of at least n=3 unless otherwise mentioned. Error bars represent S.E.M. Scale bar = 30 μm.

Figure 4: Recombinant Caspase-1 is sufficient to induce HFSC migration to the epidermis.

A. Analysis of HFSC chemotaxis to recombinant Caspase-1 proteins; wild-type (WT), catalytic dead (rCasp-1 CD) and proteolytic dead (rCasp-1 PD) in comparison to vector proteins. Mean and S.E.M. from n=2.
B. Quantification of chemotaxis in proliferating (blue) and non-proliferating (red) HFSCs to rCasp-1 CD in comparison to vector control. Mean and S.E.M. from n=3.
C. HFSC localization in Caspase-1 null skin explant treated with rCasp-1 CD and vector control. Representative images and quantification of number of HFSCs in the epidermis from 100 by 100 μm^2 boxes. Mean and S.E.M from n=2.
D. Analysis of HFSC chemotaxis to recombinant CARD and p-20 (catalytic dead) domains. Mean and S.E.M. from n=3.

Materials and Methods:

Mouse models: Caspase 8ko and Caspase-1 null: Generation of the Caspase-8 knock-out, the Caspase-1 null and the Caspase-8 knock-out/Caspase-1 null double mutant mice have been previously reported (11).

Wounding and explant experiments: 8 week old mice were wounded under isolfluorane induced anaesthesia using 5mm punch biopsy to make full thickness excisional wounds. For obtaining skin explants, 5 week old Caspase-1 null mice were sacrificed and 1 cm2 piece of skin was excised. After removal of subcutaneous fat by scraping, the explant was floated on DMEM-10% FBS media for 48 hours, with the addition of recombinant proteins. Animal work conducted in the NCBS/inStem Animal Care and Resource Center was approved by the inStem Institutional Animal Ethics Committee following norms specified by the Committee for the Purpose of Control and Supervision of Experiments on Animals, Government of India.

Cell culture and conditioned media preparation: Wild-type primary mouse keratinocyte cultures are established by isolating cells from the epidermis of newborn pups and cultured in low-calcium (0.05 mM) mouse keratinocyte media as described previously (7). For the isolation of keratinocytes and for preparation of conditioned media, Epidermis is chemically dissociated from the dermis by dispase treatment (1 hour at 37 °C) from skin of newborn pups aged p0 - p3. For primary keratinocyte isolation, the epidermis is briefly treated with 0.25% Trypsin-EDTA, followed by culturing the isolated cells on Mitomycin C treated feeder cells in low-calcium E-media (20). For preparation of epidermal conditioned media, the isolated epidermis was floated in serum-free E-media for 16 hours. HFSCs were isolated from 8 week old wild-type mice by following standard methods and cultured on feeders for 8 passages in E-media with 0.3 mM calcium (20).

Cloning, expression and purification of recombinant proteins: The murine Caspase-1 wild-type and catalytic dead constructs were gifted to us in a retroviral vector, pMScV. The genes were cloned into pET-28a vector by engineering flanking

Xho-1 and Nco-1 sites. For purification from bacterial lysates, the protein sequence was followed by C-terminal 6x-His tag expression from the vector backbone. The constructs were expressed in BL21 pLysS under IPTG induction at 18 °C for 16 hours. The cells were lysed by sonication in lysis buffer composed of 50mM Tris-HCl, 300mM NaCl, 10% glycerol, 5mM DTT, pH 8.0 with EDTA free Protease Inhibitor Cocktail, DNaseI and lysozyme. Following centrifugation at 16000g, the supernatant was incubated with Ni-NTA beads for 3 hours at 4 °C in the presence of 10mM imidazole. After washing with 20mM and 40mM imidazole, the recombinant proteins were eluted at 120mM imidazole at 4 °C in lysis buffer without additives. Following dialysis to imidazole free buffer the proteins were snap-frozen for future use. The CARD and p-20 domains were gene synthesized (Geneart, Thermo) after codon optimization with N-terminal Strep-II tag with Enterokinase cleavage site and C-terminal 10x-His tag, then cloned into pET-28a vector using the same restriction sites. Cell pellet was lysed by probe sonication in a denaturing buffer composed of 50mM Tris-HCl, pH8.0 with 6.5 M GdnHCl, 300 mM NaCl, and 50 mM imidazole; following centrifugation at 16000g, the supernatant was incubated with Ni-NTA beads. Following on-column refolding using a reducing Urea gradient in Tris-buffer with imidazole, final elution was performed at 500 mM imidazole at 4 °C. Following dialysis into imidazole-free buffer, the proteins were snap-frozen for future use. The purity of the proteins was tested by silver staining of the eluates. The concentration of the recombinant proteins was ascertained by both Bradford Reagent and quantification from silver stained gels in comparison to BSA gradient.

Chemotaxis assays and quantitation: HFSCs were trypsinized and plated onto the top chamber of either 24 well or 96 well transwell plates having 8 □m pore sizes (Corning). The conditioned media was diluted 1:3 in HFSC culture media and added to the bottom chamber. Cell migration was assayed after 12 hours of incubation when the cells were fixed by PFA and stained with Crystal Violet. The top of the transwell was cleaned before counting the cells in the bottom using the Cell Counter plugin on ImageJ. For assaying the recombinant Caspase-1, it was added to the bottom chamber at equal concentration with the vector expression protein control

(20 μg). For assaying the chemotactic potential of domains, they were added at equimolar concentration of 2.5 μM.

Histology and Immunohistochemistry: Extraction of skin after wounding and from pups, for embedding and cryosectioning was done as previously described. For explants, the skin was fixed at RT with 4% PFA, then dehydrated using a sucrose gradient of 5 – 20% in PBS, before embedding. Typically ,10 μm sections were cut.

RNA isolation and qPCR: Wound proximal tissue was obtained by using a 8mm punch biopsy tool to excise the tissue from a 5 mm punch wound. A biopsy was taken 3 cm away from the wound as unwounded tissue. Epidermal samples were collected immediately after isolation by dispase treatment. These samples were collected in chilled Trizol reagent and crushed using a tissue homogeniser (at 8000 rpm). Total RNA was extracted from crushed tissue or cell lysate using the TRIzol reagent protocol (TAKARA/Thermo). cDNA was synthesized using Superscript III (Thermo), followed by quantitative PCR using the Power SYBR mix (Life technologies) in the BioRad CFX384 machine. *Actin* or *18S* expression was used as reference for normalisation. Primer sequences used are given in Supplementary Table 1. Minimum of 3 animals of each genotype were used to obtain the data represented here as fold change ± S.E.M.

RNA Seq Data analysis: For RNA Seq reads we have taken publicly available data at NCBI repository (GEO accession ID: GSE89928) from the study by (10). The raw FASTQ files for two biological replicates, each from control and wound bulge stem cells are processed for further analysis. Briefly, the quality of FASTQ files were analyzed by FASTQC. Trimmomatic tool (21) were used to remove any adapter contamination, and high-quality reads were aligned to Mouse reference genome (GRCm38) using TopHat 2. The data were analyzed further using the “Tuxedo” pipeline: TopHat2→ Cufflinks → Cuffmerge → Cuffdiff (22). The significantly differentially expressed genes (q value < 0.05) from Cuffdiff output were used further for Gene Ontology (GO) enrichment analysis using DAVID.

Image acquisition and analysis: Fluorescent images of tissue samples were obtained on the Olympus FV1000 confocal microscope at the Central Imaging and Flow Facility at NCBS. For image processing ImageJ software was used. To analyse the distribution of HFSCs along hair follicles, the positions of Sox9+ nuclei and the the epidermis was marked manually (Fig S1) and exported to Matlab for further analysis. An in-house Matlab routine was developed to calculate the distance of the HFSCs from the epidermis along hair follicles and analyse their distribution probability from 8 μm bins starting from the epidermal line (Fig S1). The normalized probability in these bins calculated from 3 animals of each genotype has been represented as a heat-map.

Reagent list: Antibodies used for HFSC isolation are anti-CD49f-PE conjugated (BD 561894) and anti-CD34-FITC conjugated (EBiosciences, 11-0341-82). Antibodies used for immunofluorescent staining of tissues are anti-Sox 9 (Abcam, rabbit, 1:100) and anti-Keratin 5 (raised in lab, chicken, 1:100). Nuclei were stained with Hoechst. Secondary antibodies used were Alexa-488 anti-chicken (1:400) and Alexa-568 anti-rabbit (1:400) Lifetechnologies. Caspase-1 non-permeable (Cat # 400010) and cell-permeable inhibitors (Cat # 400011) were obtained from Millipore and used at a concentration of 10 μM. List of primers used for qPCR are presented in Supplementary Table 1.

Author Contributions:

S.G. conceptualized and performed experiments, evaluated and analysed data and wrote the manuscript. N.P. prepared RNA from experimental samples, and performed the gene expression analysis, A.S.A cloned, expressed and purified all the recombinant proteins, S.K. developed the image analysis routine, R.D. analysed RNA-seq data, S.P. performed cryosectioning and immunostaining, C.J. contributed to hypothesis development and manuscript preparation.

Acknowledgements:

This work is supported by the Wellcome-DBT India Alliance Early Career Fellowship awarded to Subhasri Ghosh. Animal work is supported by the National Mouse Research Resource (NaMoR) grant (102/IFD/SAN/5003/2017-2018) from DBT.

Reference:

1. Plikus, M. V, Gay, D. L., Treffeisen, E., Wang, A., Supapannachart, R. J., and Cotsarelis, G. (2012) Epithelial stem cells and implications for wound repair. *Semin. Cell Dev. Biol.* **23**, 946–53
2. Gurtner, G. C., Werner, S., Barrandon, Y., and Longaker, M. T. (2008) Wound repair and regeneration. *Nature*. **453**, 314–21
3. Ito, M., Liu, Y., Yang, Z., Nguyen, J., Liang, F., Morris, R. J., and Cotsarelis, G. (2005) Stem cells in the hair follicle bulge contribute to wound repair but not to homeostasis of the epidermis. *Nat. Med.* **11**, 1351–1354
4. Lee, P., Gund, R., Dutta, A., Pincha, N., Rana, I., Ghosh, S., Witherden, D., Kandyba, E., Macleod, A., Kobielak, K., Havran, W. L., and Jamora, C. (2017) Stimulation of hair follicle stem cell proliferation through an IL-1 dependent activation of gd T-cells. *Elife*
5. Naik, S., Larsen, S. B., Cowley, C. J., and Fuchs, E. (2018) Review Two to Tango□: Dialog between Immunity and Stem Cells in Health and Disease. *Cell*. **175**, 908–920
6. Rognoni, E., and Watt, F. M. (2018) Skin Cell Heterogeneity in Development, Wound Healing, and Cancer. *Trends Cell Biol.* **28**, 709–722
7. Lee, P., Lee, D.-J., Chan, C., Chen, S.-W., Ch'en, I., and Jamora, C. (2009) Dynamic expression of epidermal caspase 8 simulates a wound healing response. *Nature*. **458**, 519–23
8. Adam, R. C., Yang, H., Rockowitz, S., Larsen, S. B., Nikolova, M., Oristian, D. S., Polak, L., Kadaja, M., Asare, A., Zheng, D., and Fuchs, E. (2015) Pioneer factors govern super-enhancer dynamics in stem cell plasticity and lineage choice. *Nature*. **521**, 366–70
9. Nowak, J. a., Polak, L., Pasolli, H. A., and Fuchs, E. (2008) Hair follicle stem cells are specified and function in early skin morphogenesis. *Cell Stem Cell*. **3**, 33–43

10. Ge, Y., Gomez, N. C., Adam, R. C., Yuan, S., Elemento, O., Fuchs, E., Ge, Y., Gomez, N. C., Adam, R. C., Nikolova, M., Yang, H., Verma, A., Lu, C. P., Polak, L., Yuan, S., Elemento, O., and Fuchs, E. (2017) Stem Cell Lineage Infidelity Drives Wound Repair and Cancer. *Cell*. **169**, 636–642.e14
11. Lee, D.-J., Du, F., Chen, S.-W., Nakasaki, M., Rana, I., Shih, V. F. S., Hoffmann, A., and Jamora, C. (2015) Regulation and Function of the Caspase-1 in an Inflammatory Microenvironment. *J. Invest. Dermatol.* **135**, 1–31
12. Keller, M., Rüegg, A., Werner, S., and Beer, H. D. (2008) Active Caspase-1 Is a Regulator of Unconventional Protein Secretion. *Cell*. **132**, 818–831
13. Weinheimer-Haus, E. M., Mirza, R. E., and Koh, T. J. (2015) Nod-like receptor protein-3 inflammasome plays an important role during early stages of wound healing. *PLoS One*. **10**, 1–13
14. Naik, S., Larsen, S. B., Gomez, N. C., Alaverdyan, K., Sendoel, A., Yuan, S., Polak, L., Kulukian, A., Chai, S., and Fuchs, E. (2017) Inflammatory memory sensitizes skin epithelial stem cells to tissue damage. *Nature*. **550**, 475–480
15. Broz, P., and Dixit, V. M. (2016) Inflammasomes□: mechanism of assembly, regulation and signalling. *Nat. Rev. Immunol.* 10.1038/nri.2016.58
16. Roschitzki-Voser, H., Schroeder, T., Lenherr, E. D., Frölich, F., Schweizer, A., Donepudi, M., Ganesan, R., Mittl, P. R. E., Baici, A., and Grütter, M. G. (2012) Human caspases in vitro: Expression, purification and kinetic characterization. *Protein Expr. Purif.* **84**, 236–246
17. Broz, P., Von Moltke, J., Jones, J. W., Vance, R. E., and Monack, D. M. (2010) Differential requirement for caspase-1 autoproteolysis in pathogen-induced cell death and cytokine processing. *Cell Host Microbe*. **8**, 471–483
18. Ridley, A. J., Schwartz, M. a, Burridge, K., Firtel, R. a, Ginsberg, M. H., Borisy, G., Parsons, J. T., and Horwitz, A. R. (2003) Cell migration: integrating signals from front to back. *Science*. **302**, 1704–9
19. Wu, X., Shen, Q. T., Oristian, D. S., Lu, C. P., Zheng, Q., Wang, H. W., and Fuchs, E. (2011) Skin stem cells orchestrate directional migration by regulating microtubule-ACF7 connections through GSK3β. *Cell*. **144**, 341–352
20. Nowak, J. A., and Fuchs, E. (2009) Isolation and Culture of Epithelial Stem Cells.

Methods Mol. Biol. **482**, 215–232

21. Bolger, A. M., Lohse, M., and Usadel, B. (2014) Trimmomatic: A flexible trimmer for Illumina sequence data. *Bioinformatics*. **30**, 2114–2120
22. Trapnell, C., Roberts, A., Goff, L., Pertea, G., Kim, D., Kelley, R. D., Pimentel, H., Salzberg, S. L., Rinn, J. L., and Pachter, L. (2013) Differential gene and transcript expression analysis of RNA-seq experiments with TopHat and Cufflinks. *Nat. Protoc.* **7**, 562–578

Figure 1

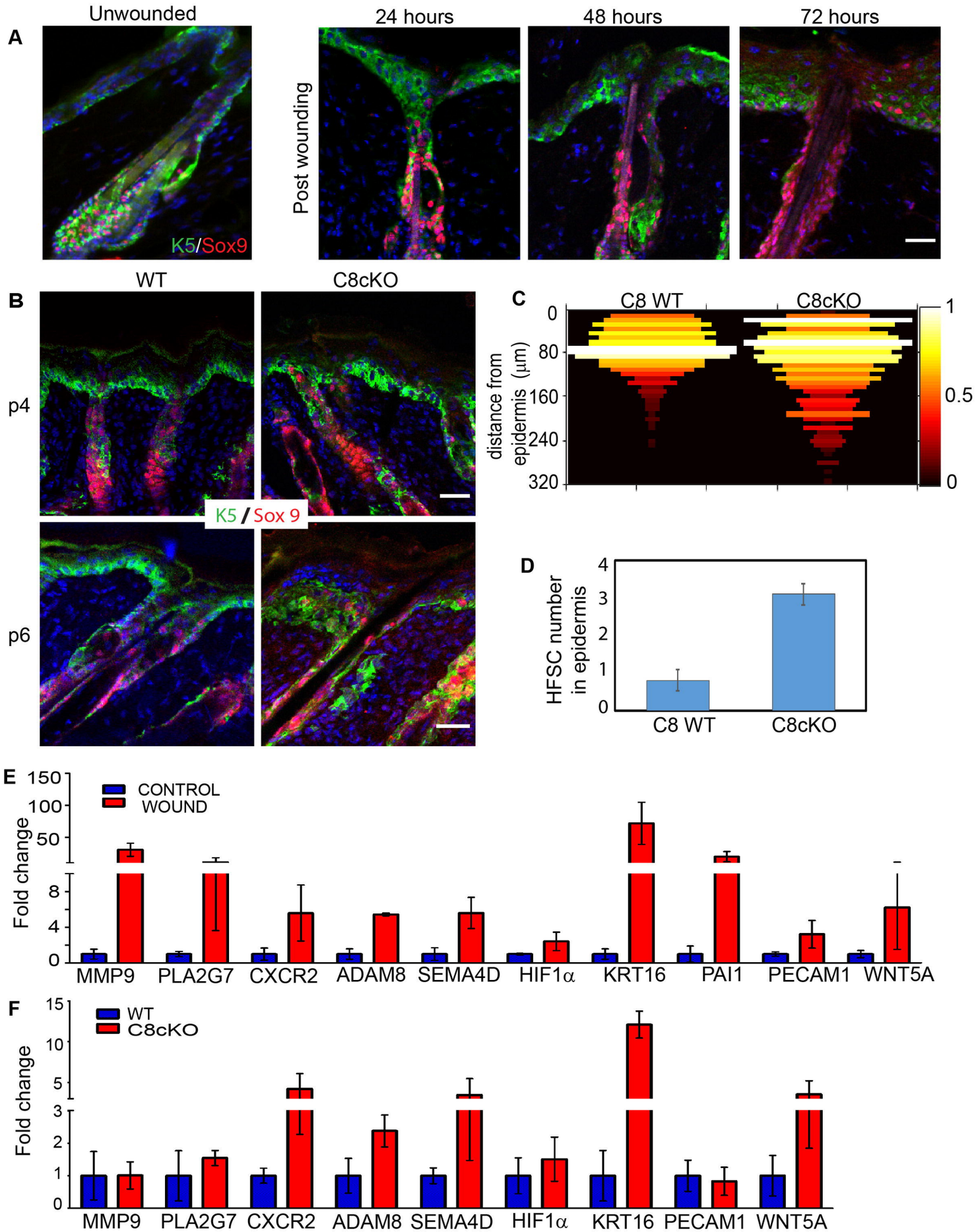
A
Unwounded
24 hours
48 hours
72 hours
Post wounding
K5/Sox9
B
WT
C8cKO
p4
p6
K5 / Sox 9
C
C8 WT
C8cKO
distance from epidermis (μm)
0
80
160
240
320
1
0.5
0
D
HFSC number in epidermis
4
3
2
1
0
C8 WT
C8cKO
E
CONTROL
WOUND
Fold change
150
100
50
8
4
0
MMP9
PLA2G7
CXCR2
ADAM8
SEMA4D
HIF1α
KRT16
PAI1
PECAM1
WNT5A
F
WT
C8cKO
Fold change
15
10
5
3
2
1
0
MMP9
PLA2G7
CXCR2
ADAM8
SEMA4D
HIF1α
KRT16
PECAM1
WNT5A

Figure 2

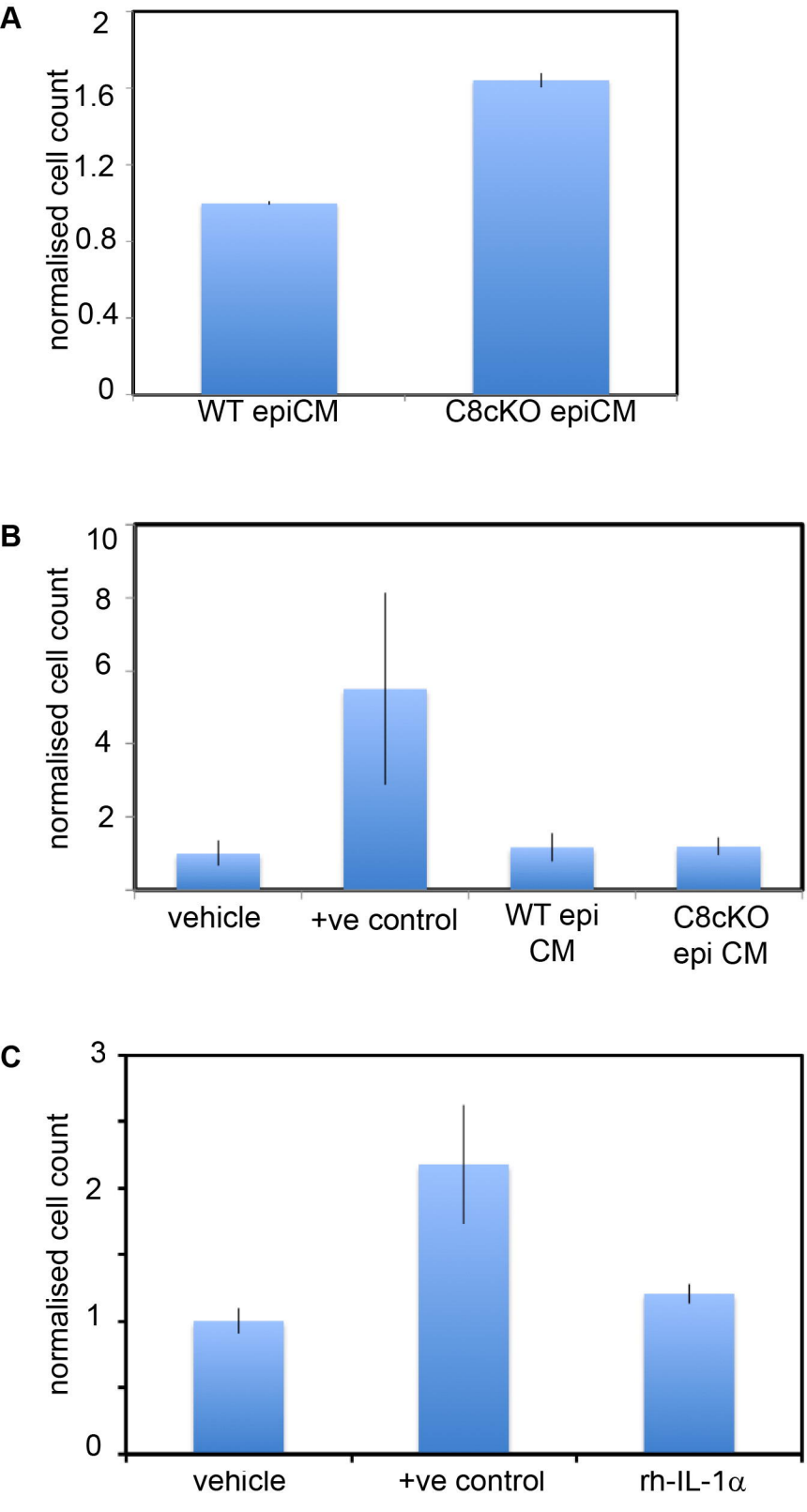
A
normalised cell count
2
1.6
1.2
0.8
0.4
0
WT epiCM
C8cKO epiCM
B
normalised cell count
10
8
6
4
2
vehicle
+ve control
WT epi CM
C8cKO epi CM
C
normalised cell count
3
2
1
0
vehicle
+ve control
rh-IL-1α

Figure 3

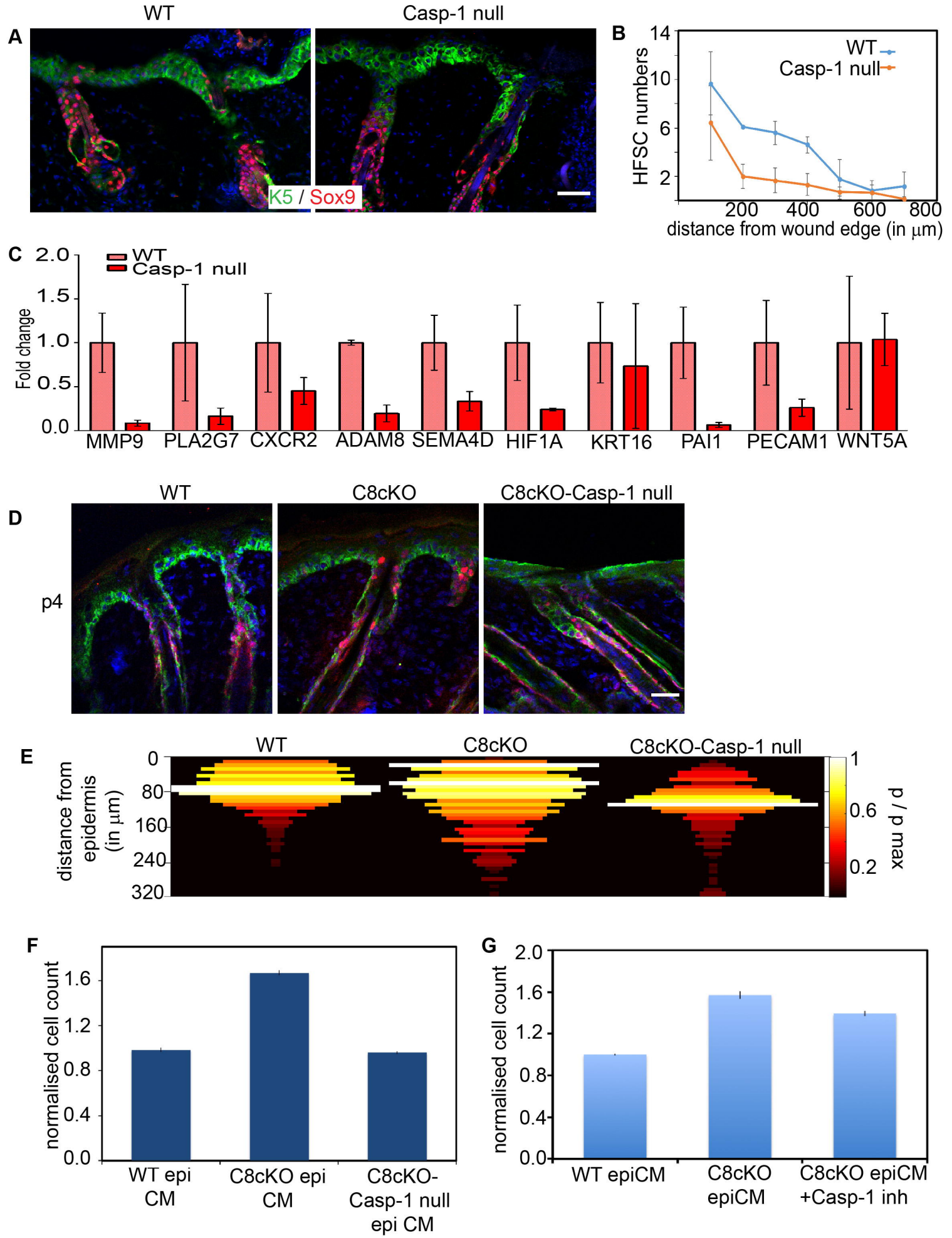
A
WT
Casp-1 null
K5 / Sox9
B
HFSC numbers
14
10
6
2
WT
Casp-1 null
200
400
600
800
distance from wound edge (in μm)
C
Fold change
2.0
1.5
1.0
0.5
0.0
WT
Casp-1 null
MMP9
PLA2G7
CXCR2
ADAM8
SEMA4D
HIF1A
KRT16
PAI1
PECAM1
WNT5A
D
WT
C8cKO
C8cKO-Casp-1 null
p4
E
WT
C8cKO
C8cKO-Casp-1 null
distance from epidermis (in μm)
0
80
160
240
320
1
0.6
0.2
p / p max
F
normalised cell count
1.6
1.2
0.8
0.4
0.0
WT epi CM
C8cKO epi CM
C8cKO-Casp-1 null epi CM
G
normalised cell count
2.0
1.6
1.2
0.8
0.4
0.0
WT epiCM
C8cKO epiCM
C8cKO epiCM +Casp-1 inh

Figure 4

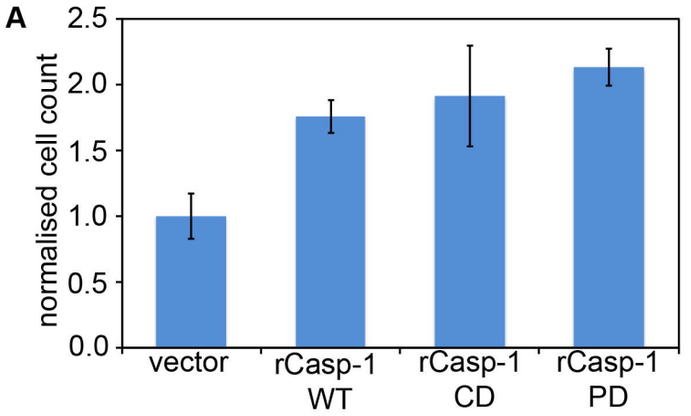
A
normalised cell count
2.5
2.0
1.5
1.0
0.5
0.0
vector
rCasp-1 WT
rCasp-1 CD
rCasp-1 PD

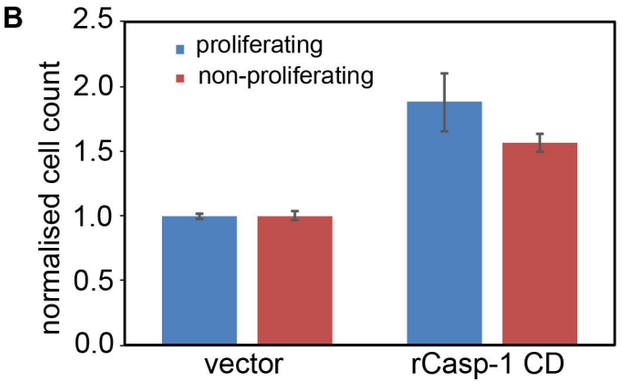
B
normalised cell count
proliferating
non-proliferating
2.5
2.0
1.5
1.0
0.5
0.0
vector
rCasp-1 CD

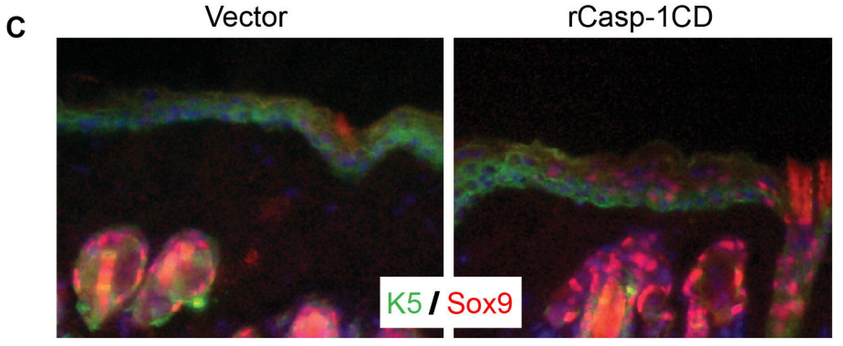
C
Vector
rCasp-1CD
K5 / Sox9

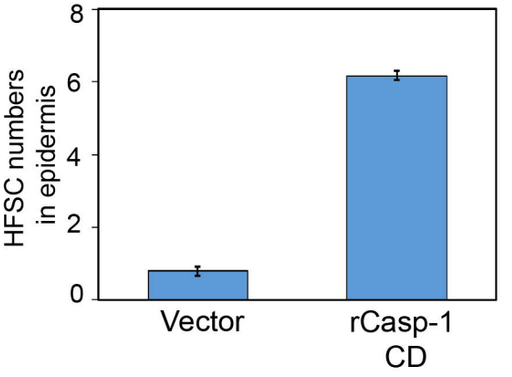
HFSC numbers in epidermis
8
6
4
2
0
Vector
rCasp-1 CD

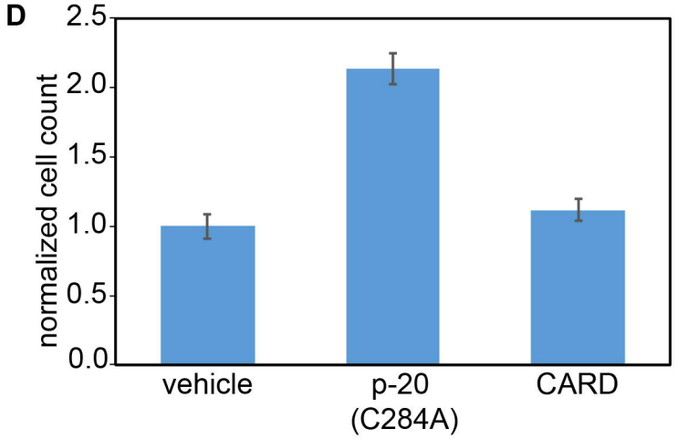
D
normalized cell count
2.5
2.0
1.5
1.0
0.5
0.0
vehicle
p-20 (C284A)
CARD